NASA TECHNICAL NOTE

NASA TN D-5169

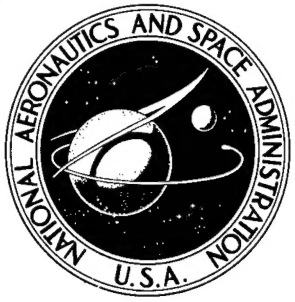

NASA TN D-5169

DYNAMIC STRAIN AGING DURING THE CREEP AND TENSILE TESTING OF A MOLYBDENUM-TITANIUM-CARBON ALLOY

by Peter L. Raffo

Lewis Research Center
Cleveland, Ohio

NATIONAL AERONAUTICS AND SPACE ADMINISTRATION • WASHINGTON, D. C. • APRIL 1969

NASA TN D-5169

DYNAMIC STRAIN AGING DURING THE CREEP AND TENSILE TESTING OF A MOLYBDENUM-TITANIUM-CARBON ALLOY

By Peter L. Raffo

Lewis Research Center
Cleveland, Ohio

NATIONAL AERONAUTICS AND SPACE ADMINISTRATION

For sale by the Clearinghouse for Federal Scientific and Technical Information
Springfield, Virginia 22151 – CFSTI price $3.00

ABSTRACT

A study was made of the influence of dynamic strain aging on the creep and short time tensile properties of a Mo-0.82 Ti-0.20 C (at. %) alloy. The strengthening effects are directly related to carbide precipitation during deformation. The precipitation lowers the density of mobile dislocations and slows down the rate of recovery.

DYNAMIC STRAIN AGING DURING THE CREEP AND TENSILE TESTING OF A MOLYBDENUM-TITANIUM-CARBON ALLOY

by Peter L. Raffo

Lewis Research Center

SUMMARY

A study was made of the creep and tensile properties of a Mo-0.82 Ti-0.20 C (at. %) alloy* in the temperature range 1800° to 3200° F (1255 to 2033 K). The experiments were aimed at characterizing the mechanism of strengthening due to the titanium and carbon additions. A peak in the flow stress-temperature curve was noted for this alloy at 1800° F (1255 K). In addition, the strain rate sensitivity of the flow stress was negative in the temperature range 1500° to 2200° F (1088 to 1477 K). The creep rate of this alloy above 2400° F (1588 K) has a stress and temperature dependence equal to that of unalloyed molybdenum. At temperatures below about 2400° F (1588 K), the creep rate at a given stress depends not only on the stress and temperature, but on the entire preloading history. Transmission electron microscopy was employed to show that precipitation occurs on dislocations in specimens crept at 1800° F (1255 K) It was deduced that the strengthening effects noted during the creep and short time tests are directly related to carbide precipitation during plastic deformation. Precipitation during deformation has two main effects. The first is associated with the decrease in the mobile dislocation density due to pinning by the carbide precipitates. Simultaneous precipitation produces logarithmic creep at temperatures higher than is found in the unalloyed metal. The decrease in the mobile dislocation density leads to a greatly decreased creep rate in a constant stress creep test and an increased work hardening rate in a constant strain rate tensile test. Secondly, precipitation during deformation may decrease the rate of recovery.

* This corresponds to the commercial Mo 0.5 Ti (wt percent) alloy.

INTRODUCTION

A strengthening effect is noted in some alloy systems which involves the diffusion of solute atoms behind moving dislocations or the simultaneous precipitation on disloca-

tions during straining. This type of effect has been variously classified as dynamic strain aging (refs. 1 and 2), strain induced precipitation (refs. 3 to 5), dynamic strengthening (refs. 6 and 7), and alloy strain aging (ref. 8). Dynamic strain aging occurs in limited temperature and strain rate ranges and is manifested by a peak in the flow stress-temperature curve (refs. 1 to 4, 6, and 9 to 11), serrated plastic flow (refs. 9 and 12 to 14), negative strain rate sensitivity of the flow stress (refs. 12, 15, and 16), and rapid rates of work hardening (refs. 5, 6, 9 to 11, 13, 14, and 17). Dynamic strain aging has been observed in many body centered cubic (bcc) alloys, particularly those which contain the interstitial solutes carbon, oxygen, and nitrogen (refs. 1 and 2). However, strengthening of this type has been observed in metals with other crystal structure (ref. 12) with both substitutional and interstitial alloying additions.

Dynamic strain aging is particularly evident in a class of molybdenum (Mo) alloys which contain carbon and group IVa carbide former such as titanium (Ti), zirconium (Zr) or hafnium (Hf) (refs. 3 to 5, and 18). All of the features peculiar to dynamic strain aging have been observed in these alloys in the temperature range of approximately 1500° to 2500° F (1088 to 1644 K). Chang (ref. 4) has studied carbide precipitation in these alloys as well as making the initial observations of dynamic strain aging. A general observation was that quenching of these alloys did not suppress the precipitation of molybdenum carbide (Mo_2C) during cooling. Upon aging at temperatures below approximately 3000° F (1922 K), the Mo_2C dissolved and precipitation of TiC or ZrC occurred, resulting in age hardening. Chang also suggested that it was the precipitation of these carbides which was responsible for the dynamic strain aging effects observed in the tensile tests.

The present work was aimed at further characterizing the mechanisms responsible for dynamic strain aging in molybenum alloys. Emphasis has been placed on the effects on creep. A commercial arc cast alloy of the composition (in at. %) Mo-0.82 Ti-0.20 C was selected for study. (This alloy is known commercially as Mo-0.5 Ti (wt. %).) Constant strain rate tensile tests at 1500° to 2400° F (1088 to 1588 K) and constant stress creep tests at 1800° to 3200° F (1255 to 2033 K) were performed on solution treated samples of this alloy.

EXPERIMENTAL PROCEDURE

The alloy Mo-0.82 Ti-0.20 C was purchased as wrought and stress relieved 0.25-inch (0.64-cm) diameter rod. The supplier quoted 2 ppm oxygen and <1 ppm nitrogen by weight as the other interstitial impurities. The rod was ground into tensile specimens having a 0.14 inch (0.36 cm) gage diameter and a 1.0 inch (2.54 cm) gage length. These specimens were employed for both constant strain rate tensile tests and creep

tests. The majority of the specimens were solution treated at 3300° F (2088 K) for 1 hour in vacuum and were rapidly cooled by introducing helium gas into the furnace. The annealing was performed in an induction furnace with a tungsten susceptor. After annealing the specimens were electropolished in a solution of 98-percent sulfuric acid in water.

Tensile tests were performed in a universal testing machine in the temperature range 1200° to 2400° F (922 to 1588 K). The specimens were heated by radiation from a resistance heated tantalum element. The tests were performed in a vacuum of less than 5×10^{-5} torr.

Constant stress creep tests in the temperature range 1800° to 3200° F (1255 to 2033 K) were performed in a vacuum of less than 5×10^{-6} torr using a resistance heated tungsten mesh heater. Constant stress conditions were met by employing either a beam similar to that described by Fullman, Carreker, and Fisher (ref. 19) or a cam of the type designed by Garafalo, Richmond, and Domis (ref. 20). A total strain of approximately 0.20 could be achieved with the beam while true strains up to 0.6 could be obtained with the cam.

The creep strain was measured optically with a cathetometer. The gage marks were small pieces of tungsten foil which were attached to the gage section of the specimen by a thin layer of tungsten powder with a glycerine binder. During the heating of the specimen, the powder sintered and firmly held the gage mark to the specimen. A change in strain of 1×10^{-4} could be detected.

Transmission electron microscopy was performed on selected crept specimens. Disks approximately 0.7 to 1 millimeter thick were spark machined from the gage length. These were glued to a brass block and ground to 0.2 to 0.4 millimeter thickness. The disks were then thinned in a solution of 14 volume percent sulfuric acid in ethyl alcohol at 8° C and 30 volts using an apparatus designed by Schoone and Fishione (ref. 21). The thinned region was subsequently examined at 100 kilovolts.

RESULTS

This portion of the paper consists of four sections. First, tensile data at constant strain rate on the Mo-Ti-C alloy are examined and shown to exhibit the previously mentioned features characteristic of dynamic strain aging. In the second section, the creep of this alloy at constant stress is described. It will be shown that above 2400° F (1588 K) the creep behavior of the alloy is much like that of unalloyed molybdenum. At 1800° F (1255 K), dynamic strain aging is found to have pronounced effects on the shape of the creep curve. These same aging effects are then shown to be exhibited during creep under constant strain (stress relaxation) in the next section. The results are then

concluded by a brief transmission electron microscopy study of the deformation substructures formed during creep.

Constant Strain Rate Tensile Tests

The effect of temperature on the ultimate tensile strength of the Mo-Ti-C alloy is shown in figure 1. Tensile data from the present study at two strain rates and from the work of Chang (ref. 3) at a single strain rate are included. In addition, results on unalloyed molybdenum (ref. 3) are plotted for comparison. Three important observations can be made from these curves. First, the combined Ti and C addition has a strengthening effect only above 1200° F (922 K). Secondly, the strength of the Mo-Ti-C alloy passes through a broad peak in the temperature range 1500° to 2100° F (1088 to 1422 K). Thirdly, the strain rate sensitivity of the flow stress is negative in this temperature region (i.e., the strength at 3.3×10^{-2} sec^{-1} is lower than that at 8.3×10^{-5} sec^{-1}).

The above characteristics of the constant strain rate tensile data on Mo-Ti-C are characteristic of a system undergoing dynamic strain aging, as indicated previously. Another characteristic, serrated stress-strain curves, was observed in the present work at 1500° F (1088 K) at a strain rate of 8.3×10^{-5} $seconds^{-1}$.

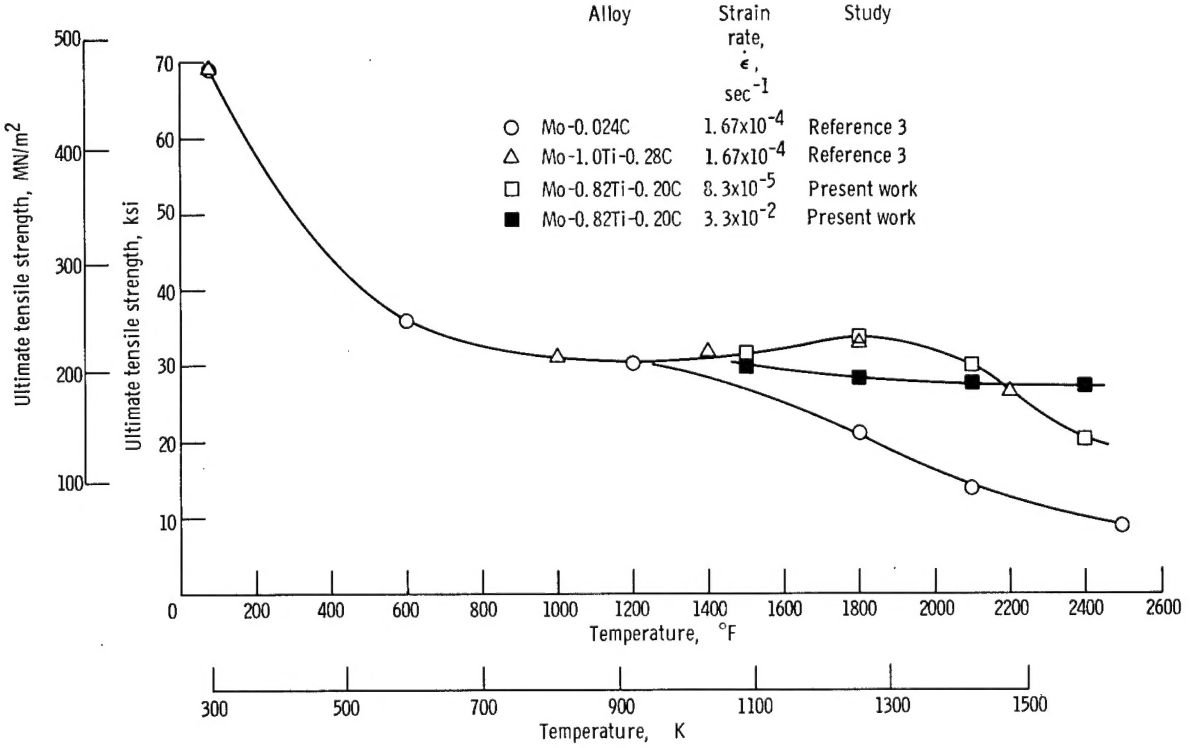

Figure 1. - Influence of temperature on ultimate tensile strength of molybdenum and Mo-Ti-C alloy.

Creep at Constant Stress

The creep behavior of the Mo-Ti-C alloy was studied at 1800° to 3200° F (1255 to 2033 K). In this section, the data are presented in two parts. First, creep data for tests above 2400° F (1588 K) are presented. These data are shown to be typical of the creep of pure metals. The second part describes a study of creep at 1800° F (1255 K) where dynamic strain aging (DSA) effects are apparent during incremental testing.

Creep at 2400° to 3200° F (1588 to 2033 K). - Constant stress creep tests at 2400° to 3200° F (1588 to 2033 K) were performed on specimens annealed at 3300° F (2088 K). The creep curves at these temperatures showed a small amount of primary creep, generally less than 1 percent, followed by a well-defined linear steady-state region. The small transient creep strain allowed measurement of the creep rate at more than one stress on the same specimen. The steady-state creep rates $\dot{\epsilon}_s$ which were obtained are given in table I.

The stress dependence of the steady-state creep rate $\dot{\epsilon}_s$ is plotted in figure 2. The creep rates and the stresses are compensated for temperature in the manner suggested by Sherby and Burke (ref. 22). This is accomplished by dividing the creep rate by the self-diffusion coefficient of molybdenum and the stress by the value of Young's modulus at temperature. The diffusion coefficient D taken from Askill and Tomalin (ref. 23) was given as

TABLE I. - CREEP DATA ABOVE 2400° F (1588 K)

[All specimens preannealed for 1 hr at 3300° F (2088 K).]

Temperature		Stress, σ		Steady-state creep rate, $\dot{\epsilon}_s$, sec^{-1}
°F	K	ksi	MN/m^2	
2400	1588	7.0	48.3	1.3×10^{-7}
		8.3	57.2	5.6
		10.8	74.5	1.6×10^{-6}
		12.8	88.3	2.3
3000	1922	2.9	20.0	9.0×10^{-7}
		4.7	32.4	7.9×10^{-6}
3200	2033	1.6	4.1	6.4×10^{-7}
		1.7	4.8	7
		2.1	14.5	1.6×10^{-6}
		2.5	17.2	6.1

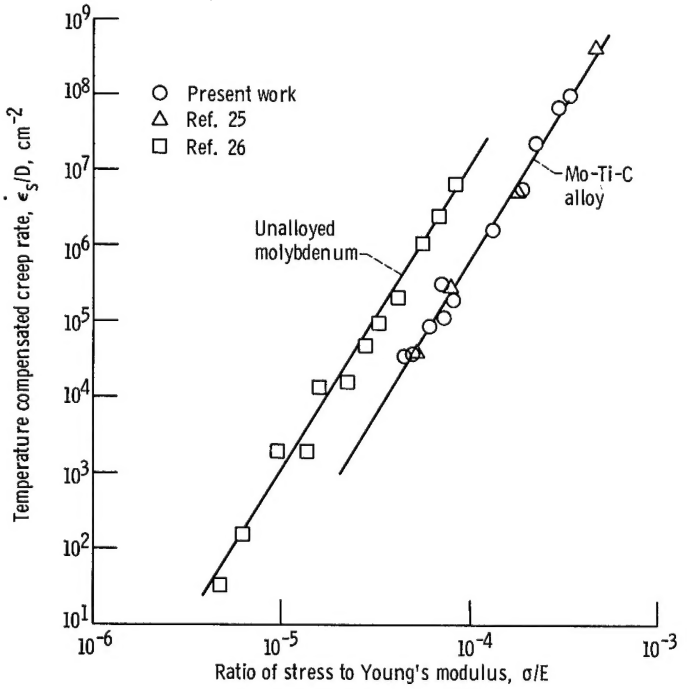

Figure 2. - Low stress creep of molybdenum (ref. 26) and Mo-Ti-C alloy (present work and ref. 25).

$$D = 0.5 \exp(-96\,900\ RT)$$

The modulus values were those of Armstrong and Brown (ref. 24). Figure 2 also includes some constant load data on a similar alloy from Semchyshen, et. al., (ref. 25) at 2400° F (1588 K). In addition to the results on the Mo-Ti-C alloy, the creep rates for unalloyed molybdenum from the work of Flagella (ref. 26) are plotted for comparison with the alloy.

The temperature compensated creep rate $\dot{\epsilon}_s/D$ was proportional to $(\sigma/E)^4$ for both unalloyed molybdenum and our Mo-Ti-C alloy.[1] This behavior is in common with pure metals at less than $\dot{\epsilon}_s/D = 10^9$ centimeters^{-2} (ref. 22). At a given value of σ/E, the creep rate of the alloy is about one order of magnitude less than that of the pure metal.

Creep at 1800° F (1255 K). - Although the creep behavior of the Mo-Ti-C alloy is much like that of a pure metal above 2400° F (1588 K), distinct effects appear in the creep curve below this temperature which are evidently due to dynamic strain aging. Figure 3 shows an example of this behavior. Curve A is for a specimen crept at 1800° F

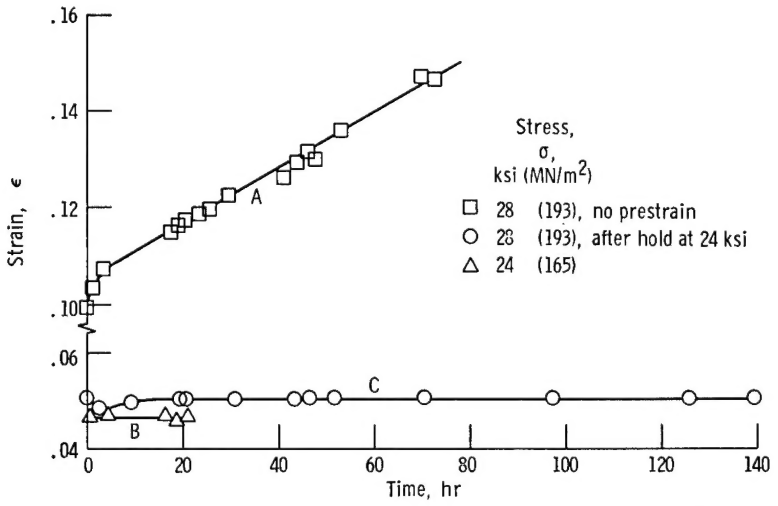

Figure 3. - Influence of prestrain of 24 kips per square inch (165 MN/m^2) on creep at 1800° F (1255 K).

(1255 K) at a stress of 28 ksi (193 MN/m^2). A steady-state region is observed for close to 75 hours after a large initial strain of approximately 0.10 and a small transient. The steady-state creep rate was 1.6×10^{-7} second^{-1}. Curve B in figure 3 represents the

[1] Flagella (ref. 26) computed a stress dependence of five for his data on unalloyed molybdenum using the same approach. His data were subjected here to the same least-squares analysis used for the Mo-Ti-C alloy, and the result was the stress dependence of four quoted here.

creep behavior of another specimen after stressing at 24 ksi (165 MN/m^2) for 24 hours. After an initial strain of 0.046, no creep was observed. Upon increasing the stress on this specimen to 28 ksi (193 MN/m^2) (curve C), the creep rate was observed to be zero for the next 140 hours, with the exception of a small transient which involved some contraction. This behavior should be compared with curve A, where the 28 ksi (193 MN/m^2) was applied without the prestress at 24 ksi (165 MN/m^2). It appeared that the zero creep rate at 28 ksi (193 MN/m^2) was due to precipitation which occurred specifically during straining at the lower stress. This strain aging can be contrasted with the lack of aging noted in unstressed samples of similar alloys by Chang (ref. 4).

It was decided to study effects such as those in figure 3 during creep at 1800° F in more detail. The experimental procedure is diagrammed in figure 4. A specimen was initially loaded to σ_o = 20 ksi (138 MN/m^2) and crept under that stress for a time t_a. At t_a, the stress is increased by an amount $\Delta\sigma_a$ and crept again for t_a. The stress is then increased to $\sigma_o + 2\Delta\sigma_a$ ksi and the whole process is repeated. The creep behavior during this loading program was examined for t_a = 0.5 and 24 hours and $\Delta\sigma_a$ = 2, 4, or 8 ksi (14, 28, or 56 MN/m^2).

The creep behavior at 1800° F (1255 K) depended strongly on the magnitude of t_a and $\Delta\sigma_a$. The creep rate at a stress greater than σ_o tended to be smaller if the time t_a was longer or if the stress increment $\Delta\sigma_a$ was decreased.

An important observation was made concerning the shape of the creep curve during the time period t_a. Rather than the normal linear behavior which was evidenced by curve A in figure 3, the creep curve followed an equation of the form

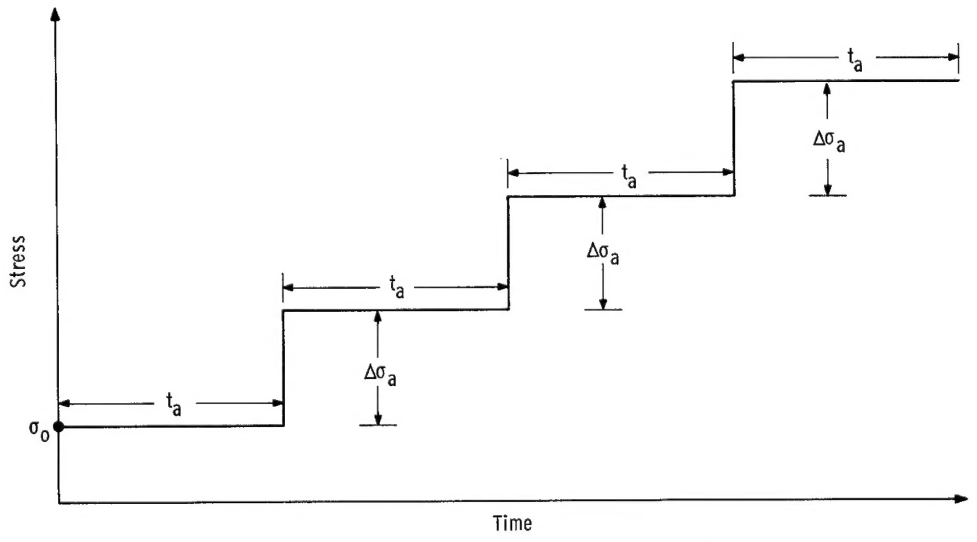

Figure 4. - Schematic of loading program used in incremental creep tests at 1800° F (1255 K), where t_a is time under given creep stress and $\Delta\sigma_a$ is change in stress during incremental creep test.

$$\epsilon = A + \alpha \ln(t + t_o) \tag{1}$$

where A, α, and t_o are constants. This type of creep behavior is termed logarithmic creep and is usually observed in pure metals and alloys below 0.3 T_m, where T_m is the melting point (ref. 27). Typical logarithmic creep curves are shown in figure 5 for one specimen which was loaded under the conditions $\Delta\sigma_a$ = 2.0 ksi, t_a = 24 hours. The observance of logarithmic creep is unusual at this high a temperature (1800° F equals 0.41 T_m for molybdenum). It will be shown in a later section that its presence can be related to dynamic strain aging.

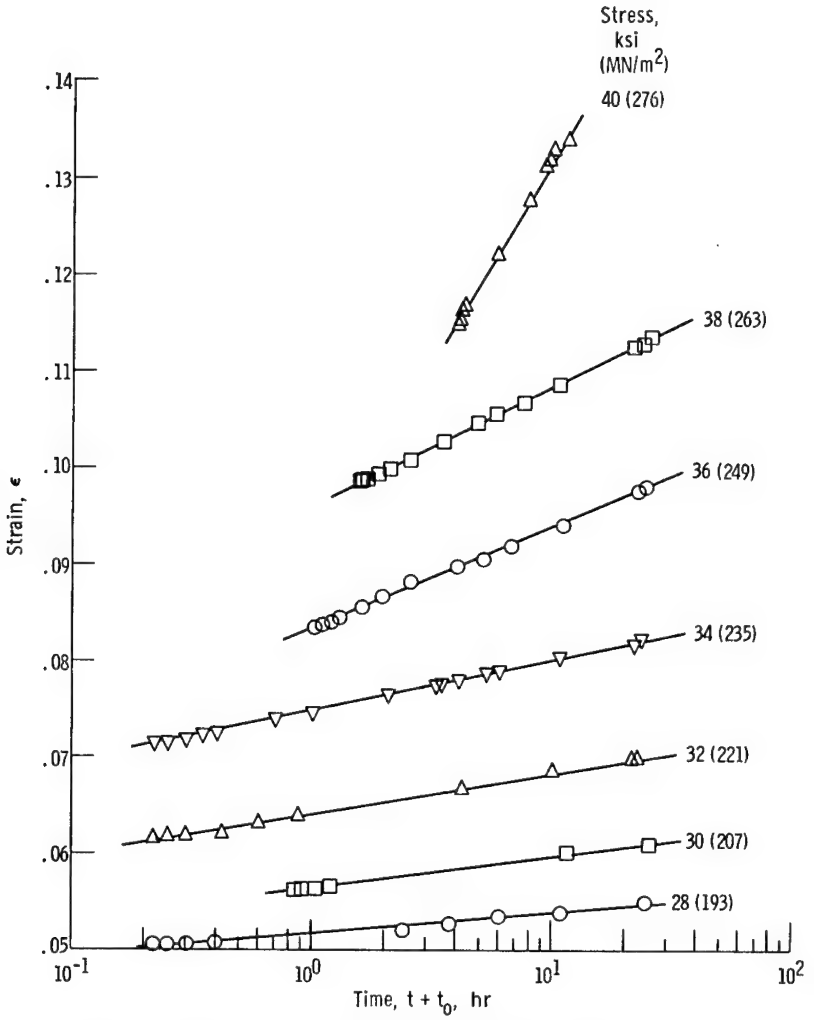

Figure 5. - Logarithmic creep of Mo-Ti-C alloy at 1800° F (1255 K). Time under given creep stress, 24 hours; change in stress during incremental creep test, 2 kips per square inch (14 MN/m²).

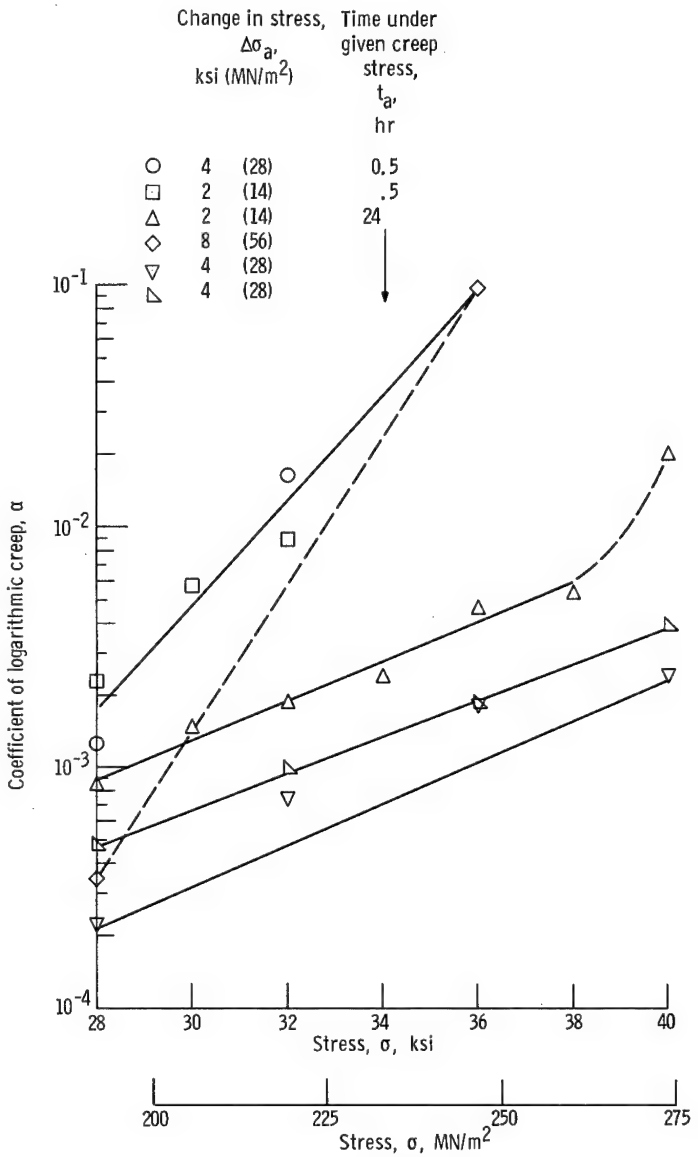

Figure 6. - Stress dependence of logarithmic creep constant α for different loading histories.

The variation of the logarithmic creep constant α with stress is shown in figure 6 for various combinations of $\Delta\sigma_a$ and t_a. The points for $t_a = 0.5$ hour appear to fall on one curve with a slope larger than those observed for $t_a = 24$ hours. The data for $\Delta\sigma_a = 8$ ksi and $t = 24$ hours appear to fall on a line with a much larger slope (dashed line in fig. 6). The data for stresses less than 28 ksi were not plotted in figure 6, as the creep rates are too low for an accurate determination of α. The other constant in equation (1) also increased with increasing stress but the variation with stress did not follow a consistent pattern.

An experiment was also performed to see if the creep rate could be affected by altering the distribution of solute in the alloy. One specimen was solution treated at 3300° F (2088 K) as before and then overaged at 2800° F (1810 K) for 16 hours. The specimen was then cooled slowly (in 2 hr) to the test temperature 1800° F (1255 K) to try to avoid any supersaturation. At this point, the stress σ_o = 20 ksi was applied as before, and the specimen was tested with $\Delta\sigma_a$ = 4 ksi and t_a = 24 hours. The results are shown in figure 7 with the data for the solution treated alloy for comparison. It is obvious that decreasing the potential for precipitation during creep by overaging substantially increases the creep rate at a given time and stress.

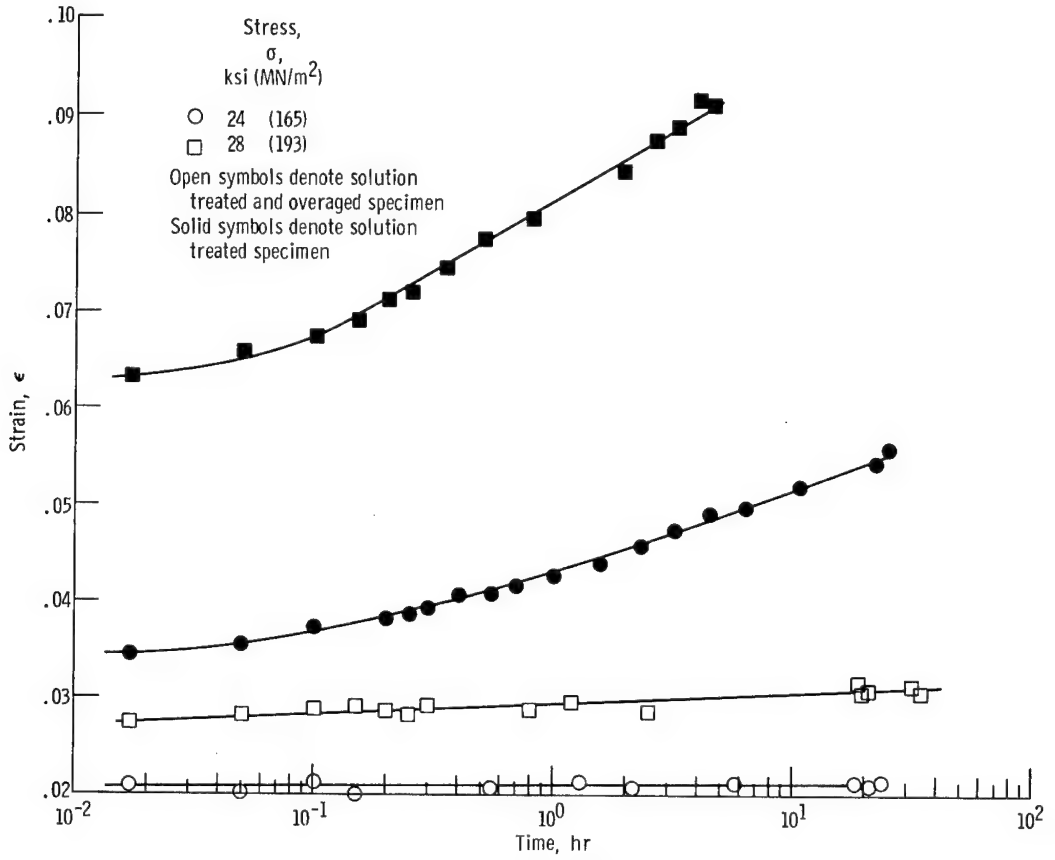

Figure 7. - Effect of overaging on creep behavior at 1800° F (1255 K).

Creep Under Constant Strain

In the previous section, creep tests were described which showed what appeared to be strain aging during creep. A limited number of tests were also performed under

constant strain conditions (stress relaxation) to study the change in flow stress produced by aging under these conditions. This type of study has been previously used to good advantage by Rosen and Bodner (refs. 15 and 16) and Owen and Roberts (ref. 28) in studies of dynamic strain aging in aluminum and martensitic steels, respectively.

The test procedure is given schematically in figure 8. A specimen was strained in tension at 8.3×10^{-4} second^{-1} to a stress σ_1 above the yield stress, at which time the crosshead is stopped. The load is then allowed to relax for a time t_r to a stress σ_r

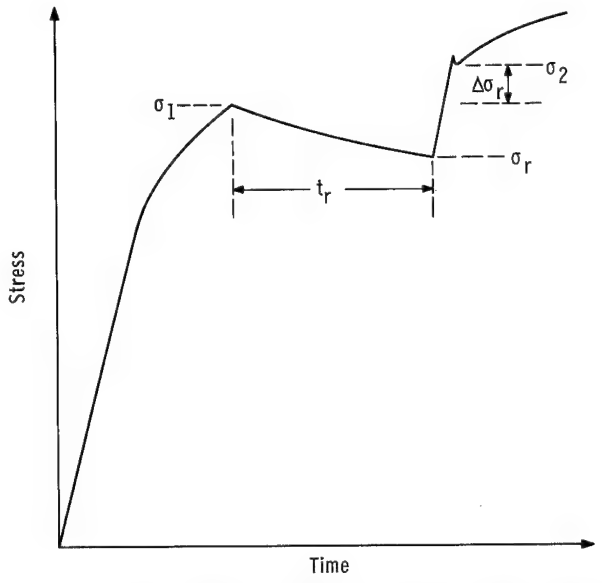

Figure 8. - Schematic of relaxation experiment showing definition of terms, where t_r is relaxation time, σ_1 is initial stress in stress relaxation test, σ_2 is yield stress on reloading after stress relaxation, σ_r is stress at time t_r, and $\Delta\sigma_r = \sigma_2 - \sigma_1$.

during which time the specimen creeps under essentially constant strain conditions. The crosshead is then restarted and the specimen reyields at a stress σ_2. The stress increment $\Delta\sigma_r = \sigma_2 - \sigma_1$ is then recorded and the entire process is repeated. The sign of $\Delta\sigma_r$ may be positive or negative.

Figure 9 shows the variation of $\Delta\sigma_r$ with strain for a relaxation time t_r = 30 seconds at various temperatures. Initially, $\Delta\sigma_r$ was always positive and a distinct yield point was observed on restraining as indicated in figure 8. The value of $\Delta\sigma_r$ decreased with increasing strain until a specific strain ϵ_c when $\Delta\sigma_r$ became negative. At 1500° F (1088 K), $\Delta\sigma_r$ first passed through a maximum before decreasing. The critical strain was dependent on temperature; lower temperatures gave a higher value of ϵ_c.

The negative values of $\Delta\sigma_r$ probably result from recovery processes occurring during the relaxation. We define the term recovery to be any process which would tend to lower the flow stress from its initial value at σ_1. The recovery of the flow stress occurs simultaneously with the increase in the flow stress produced by aging. As the

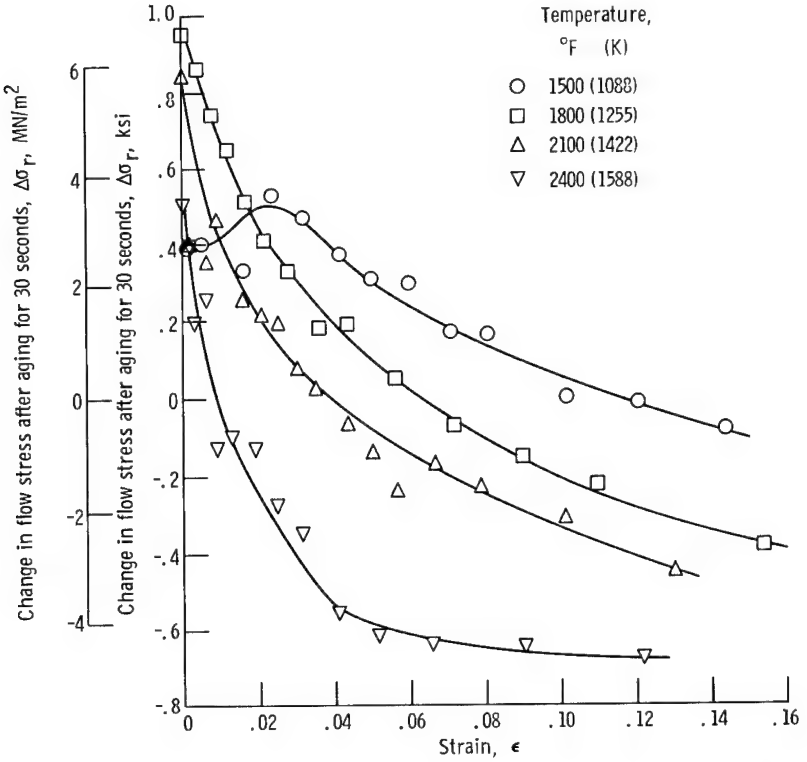

Figure 9. - Stress increment $\Delta\sigma_r$, after aging under constant strain for 30 seconds, as function of strain and temperature.

temperature is increased, recovery is more rapid and tends to overwhelm the aging process at lower strains. This resulted in the decrease in ϵ_c with increasing test temperature. An attempt was also made to determine the time dependency of $\Delta\sigma_r$ at 1500° F (1088 K) and 2100° F (1422 K). The results were very erratic, suggesting that the simultaneous recovery and aging processes have different time dependencies.

The importance of the stress relaxation tests is that the simultaneous processes of aging and recovery are observed. The presence of recovery is not as obvious in the creep tests as it is in the relaxation tests.

Transmission Electron Microscopy

The purpose of this section is to characterize, with the use of transmission electron microscopy (TEM), the dislocation substructures formed during creep straining. Thin foils were viewed from selected specimens crept at 1800° F (1255 K), where dynamic strain aging is thought to play a role, and at temperatures from 2400° to 3200° F (1588 to 2033 K) as well. A structure typical of creep above 2400° F (1588 K) is shown in figure 10. The structures generally consisted of well developed subgrains with few dis-

Figure 10. - Microstructure of specimen crept at 3200° F (2033 K) at stress of 2.5 kips per square inch. (17.2 MN/m^2). X30 000.

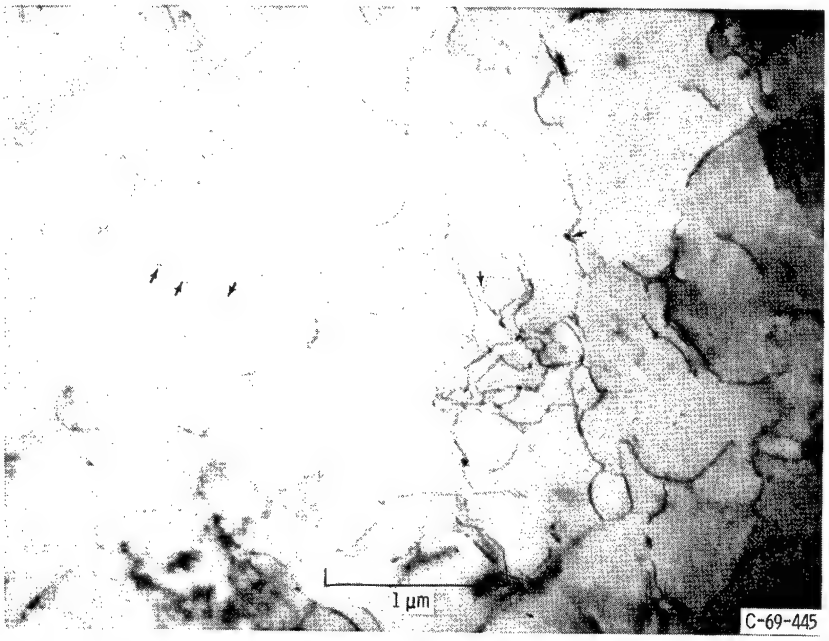

Figure 11. - Transmission electron micrograph taken from specimen tested at 1800° F (1255 K). Prestrained at 24 kips per square inch (165 MN/m^2) for 24 hours and then tested at 28 kips per square inch (193 MN/m^2) see figure . Arrows indicate selected precipitates on dislocations. X50 000.

locations within the subgrains. This structure is typical of that shown previously by other investigators on crept or recovered bcc metals (ref. 29). The only carbide precipitates observed were a few widely spaced 0.5 to 1 micron particles and the previously mentioned grain boundary carbide precipitates.

The substructures of the specimens crept at 1800° F (1255 K) showed important differences when compared to those formed at the higher temperatures. Precipitation on dislocations was readily seen in all conditions, while it was not apparent in the specimens crept above 2400° F (1588 K). The precipitates were generally observed as a widening in the dislocation lines, as indicated by the arrows in figure 11. The creep curve of the specimen pictured in figure 11 was previously shown in figure 3, curve C.

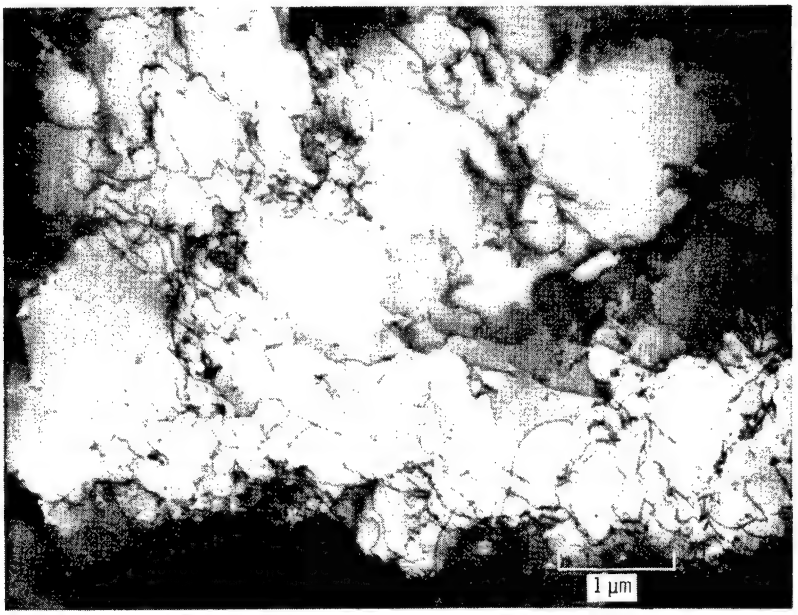

(a) Change in stress, $\Delta\sigma_a$ = 4 kips per square inch (28 MN/m^2).

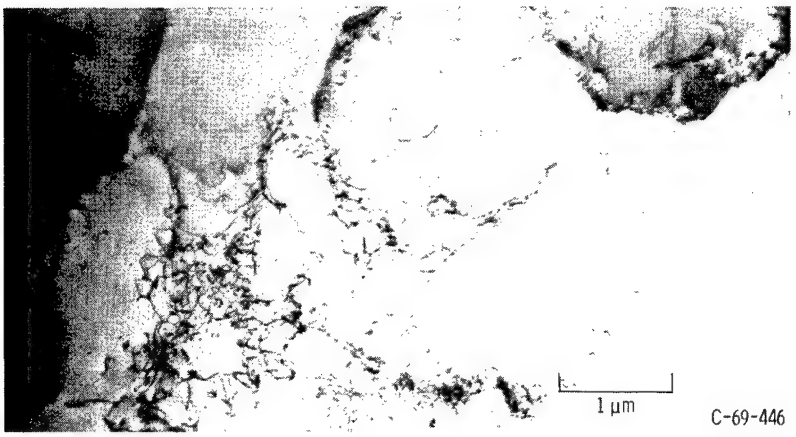

(b) Change in stress, $\Delta\sigma_a$ = 8 kips per square inch (56 MN/m^2).

Figure 12. - Microstructures after creep at 1800° F (1255 K) under two different loading programs. Time under given creep stress, 24 hours. X30 000.

The size of the precipitates was difficult to measure, but where a widening in the line was observed, it had an apparent diameter of approximately 200 Å. This represents an upper limit to their size.

Another important feature was the effect of the loading history produced by different combinations of $\Delta\sigma_a$ and t_a on the dislocation substructure. Examples are shown in figures 12(a) and (b). Figure 12(a) shows the structure of a specimen which had been loaded for 24 hour periods with a $\Delta\sigma_a$ of 2 ksi. Figure 12(b) shows a specimen similarly loaded but with $\Delta\sigma_a$ = 8 ksi. A cell structure was formed in each case, but for $\Delta\sigma_a$ = 8 ksi the region within the cells had a lower dislocation density. Precipitation on dislocations was observed in all of the specimens crept at 1800° F (1255 K), regardless of the loading history.

DISCUSSION

The preceding sections have illustrated that dynamic strain aging occurring both in constant stress creep tests and in constant strain rate tensile tests of the molybdenum alloy Mo-0.82 Ti-0.20 C. The DISCUSSION section presents a rationale for these observations, leading to the conclusion that precipitation during deformation accounts for the effects.

Aging Effects During Creep

Three important observations were made concerning the creep of the Mo-Ti-C alloy at 1800° F (1255 K). First, the creep at this temperature was dependent on the loading history. Secondly, the creep curve at a given stress was logarithmic in shape. Finally, the creep rate at a given stress could be substantially increased by a prior aging treatment which removed the potential for precipitation during the creep tests.

The effects of aging on the creep curve are discussed using a dislocation dynamics approach developed by Li (ref. 30) and others. The theory is modified somewhat in the present work to account for simultaneous precipitation. The approach taken by Li assumes that the creep rate at a given time arises from the simultaneous production and immobilization or annihilation of mobile dislocations. The production of mobile dislocations may result from multiplication by a double cross slip or dipole crossover mechanism. The immobilization may result by either annihilation of dislocations of opposite sign or by their becoming held up indefinitely in a tangle.

Li then assumes that the decrease in the creep rate $\dot{\epsilon}$ during transient creep is due to a decrease in the mobile dislocation density only. The time rate of change of the

mobile dislocation density $\dot{\rho}$ is assumed to be composed of two terms $\dot{\rho}_1$ and $\dot{\rho}_2$. The first term $\dot{\rho}_1$ represents the rate of increase in ρ due to dislocation multiplication. The second term $\dot{\rho}_2$ represents a rate of decrease in ρ due to annihilation of dislocations of opposite sign. The term $\dot{\rho}_1$ is presumed to follow first order kinetics while the kinetics of the annihilation process leading to $\dot{\rho}_2$ are of second order. The net rate of change of the mobile dislocation density may be written as

$$\dot{\rho} = \dot{\rho}_1 - \dot{\rho}_2 = k_1\rho - k_2\rho^2 \tag{2}$$

where k_1 and k_2 are rate constants which vary with stress and temperature.

We would like to add another term $\dot{\rho}_p$ to equation (2) which takes into account the immobilization of dislocations due to pinning by precipitates. We will also assume that $\dot{\rho}_p$ will follow first order kinetics. This results from $\dot{\rho}_p$ probably being a function of the rate of nucleation of precipitates on dislocations which is proportional to the total number of dislocations present (ref. 31). Thus,

$$\dot{\rho}_p = -k_p\rho \tag{3}$$

and equation (2) becomes

$$\dot{\rho} = (k_1 - k_p)\rho - k_2\rho^2 \tag{4}$$

where k_p is now a rate constant relating to probability of nucleation of precipitates on dislocations. This equation is of the same form as equation (2), and following the method of Li (ref. 30) it may be integrated and substituted into the strain rate equation

$$\dot{\epsilon} = b\rho\bar{v} \tag{5}$$

where b is the Burger's vector and $\bar{v}$ is the average dislocation velocity. Equation (5) is now integrated to find the strain-time relation (i.e., the creep curve)

$$\epsilon = \epsilon_o + \frac{\dot{\epsilon}_s}{k_1 - k_p} \ln\left[1 + \frac{\dot{\epsilon}_i - \dot{\epsilon}_s}{\dot{\epsilon}_s}\left(1 - e^{-(k_1-k_p)t}\right)\right] + \dot{\epsilon}_s t \tag{6}$$

where ϵ_o is the initial strain and $\dot{\epsilon}_i$ and $\dot{\epsilon}_s$ are the initial and steady-state creep rates, respectively.

By making certain assumptions as to the relative magnitudes of $\dot{\epsilon}_i$, $\dot{\epsilon}_s$ and $k_1 - k_p$ in equation (6) more familiar forms of the creep curve may be derived. For example,

if the initial creep rate $\dot{\epsilon}_i$ is very much greater than the final steady-state creep rate $\dot{\epsilon}_s$ and the value of $(k_1 - k_p)t$ is small, equation (6) reduces to

$$\epsilon = \epsilon_o + \frac{\dot{\epsilon}_s}{k_1 - k_p} \ln \frac{\dot{\epsilon}_i(k_1 - k_p)}{\dot{\epsilon}_s} + \frac{\dot{\epsilon}_s}{k_1 - k_p} \ln \left[t + \frac{\dot{\epsilon}_s}{\dot{\epsilon}_i(k_1 - k_p)} \right] \tag{7}$$

This is the logarithmic form which was found for the creep curves in figure 5 and given in equation (1). The empirically derived constants in equation (1) are related to the theoretical parameters in equation (7) by

$$A = \epsilon_o + \frac{\dot{\epsilon}_s}{k_1 - k_p} \ln \frac{\dot{\epsilon}_i}{\dot{\epsilon}_s} (k_1 - k_p) \tag{8a}$$

$$\alpha = \frac{\dot{\epsilon}_s}{k_1 - k_p} \tag{8b}$$

$$t_o = \frac{\dot{\epsilon}_s}{\dot{\epsilon}_i(k_1 - k_p)} \tag{8c}$$

The preceding results suggested that low rates of dislocation multiplication and rapid rates of precipitation on dislocations can lead to logarithmic creep. These factors produce the low value of the difference $k_1 - k_p$ allowing the general creep equation (eq. (7)) to reduce to the logarithmic form.

It is impossible to decide which of the two rate constants k_1 or k_p is the more important since they always appear together in the creep equation. The other constant k_2 expresses the rate of annihilation of dislocations of opposite sign. This should be proportional to the rate of dislocation climb which would be small at this temperature in molybdenum (0.41 T_m). We can, however, make some general comments on the effects of loading history on the creep behavior at 1800° F (1255 K). Precipitation does occur on dislocations during creep. This was observed in the micrograph in figure 11. If sufficient precipitation occurs, the dislocations will become immobilized at a given stress. We will assume that a dislocation becomes immobilized when the spacing between particles L along a dislocation line is given by (ref. 32)

$$L < \frac{2\mu b}{\sigma} \tag{9}$$

where μ is the shear modulus and b is the Burger's vector. For stresses ranging from 20 to 40 ksi (138 to 276 MN/m^2) as in this experiment, the calculated value of L is approximately 0.2 to 0.4 micron. The particle spacing in figure 11 is significantly smaller than this, indicating that these dislocations are pinned. An additional effect of immobilization is to prevent the dislocations from eventually acting as sources of additional mobile dislocations. The effect of increasing t_a on the creep rate in the succeeding stress is to allow time for greater amount of precipitation and thus to promote more complete immobilization.

It was observed that the creep rate at a given stress was also dependent on the magnitude of the stress increment used to reach that stress. This can be rationalized by assuming that there is a range of particle spacings along the dislocations. Thus, increasing the stress by $\Delta\sigma_a$ may activate portions of the dislocation network where the particle spacing is greater than $2\mu b/\sigma$. Increasing the stress increment would thus make possible the reactivation of a larger percentage of the dislocations immobilized at the previous stress. For low stress increments there should also be a greater number of pinned dislocations since the number mobilized at each new stress increment is small. This would explain the larger dislocation density seen in the specimen strained with $\Delta\sigma_a$ = 4 ksi compared to that strained with $\Delta\sigma_a$ = 8 ksi in figure 12.

The Relation Between Dynamic Strain Aging in Creep and Under Constant Strain Rate Conditions

A simple phenomenological approach has been used in the previous section to explain the aging effects during creep observed during this work. Most of the previous studies on dynamic strain aging in metal systems (ref. 1) have been performed using constant strain rate tests. It is thus important at this time to compare the effects of aging in the two types of tests.

This comparison can be best discussed with the strain rate equation

$$\epsilon = \rho b \bar{v}$$

At constant stress, a good assumption is that $\bar{v}$ does not change throughout the test so that the creep rate is controlled by the mobile dislocation density only. The effect of aging during deformation is thus to produce a more rapid decrease in the creep rate than if the precipitation did not take place. Constant strain rate, however places a restriction on the deformation process so that the details of the strengthening due to aging are different. This restriction is that the product $\rho\bar{v}$ must remain constant during the test. Since ρ will have a tendency to decrease as precipitation occurs, the dislocation

velocity and therefore the stress must increase to maintain the applied strain rate. Two effects may occur as the stress increases. If the pinning is weak, dislocations may break away, producing more mobile dislocations. If the pinning is strong enough, new dislocation sources may begin to operate to produce fresh dislocations. The number of new sources operating produces a more rapid increase in the total dislocation density than if precipitation did not occur. Rapid rates of dislocation multiplication have been measured in a number of systems undergoing dynamic strain aging (ref. 1). It has been shown that it is this increase in the total dislocation density which produces the strengthening and consequently the observed peak in the flow stress-temperature curve (refs. 13 and 14).

Retardation of Recovery in Mo-Ti-C Alloy

The decrease in the strain ϵ_c with decreasing temperature in the relaxation tests in figure 9 attests to the fact that the aging and recovery processes occur simultaneously. It appears that the precipitation during the creep and tensile tests may also retard recovery by perhaps pinning dislocation networks or some other portion of the dislocation substructure. This has been suggested by Wilcox and Allen (ref. 6) as a mechanism for the low deformation rates in Cb-Zr-O alloys.

This retardation of recovery may also account for the small increase in the creep strength of molybdenum conferred by titanium and carbon above 2400° F (1588 K). It was shown in figure 2 that alloying did not change the basic mechanism of creep of molybdenum since the activation energy and stress dependence were not altered. Precipitation on dislocations was not observed at high temperatures so that any recovery inhibition must take place by another mechanism. This may occur by clusters of titanium and carbon atoms pinning the dislocation network. These clusters would then be too small to be observed by transmission electron microscopy. Clustering of manganese and nitrogen atoms has been proposed by Ishida and McLean (ref. 33) to explain the retardation of recovery during the creep of an Fe-Mn-N alloy.

CONCLUSIONS

A study of creep and dynamic strain aging in a Mo-Ti-C alloy led to the following conclusions:

1. The strengthening effects during the creep and short time tensile tests of a Mo-Ti-C alloy are directly related to precipitation during plastic deformation.

2. Precipitation during deformation has two main effects. The first is associated with the decrease in the mobile dislocation density due to pinning by the carbide precipitates. Secondly, precipitation during deformation may decrease the rate of recovery.

Lewis Research Center,
National Aeronautics and Space Administration,
Cleveland, Ohio, January 31, 1969,
129-03-02-08-22.

APPENDIX - SYMBOLS

A	constant in logarithmic creep equation
b	Burger's vector
D	self-diffusion coefficient
E	Young's modulus
k_1, k_2, k_p	rate constants
T_m	melting point
t	time
t_a	time under given creep stress
t_o	constant in logarithmic creep equation
t_r	relaxation time
$\bar{v}$	average dislocation velocity
z	rate constant
α	constant in logarithmic creep equation
ϵ	strain
ϵ_c	critical strain
ϵ_o	initial strain
$\dot{\epsilon}$	strain rate
$\dot{\epsilon}_i$	initial strain rate
$\dot{\epsilon}_s$	steady-state creep rate
ρ	mobile dislocation density
$\dot{\rho}$	time dependence of mobile dislocation density
σ	stress
σ_o	initial stress
σ_r	stress at time t_r
σ_1	initial stress in stress relaxation test
σ_2	yield stress on reloading after stress relaxation
$\Delta\sigma_a$	change in stress during incremental creep test
$\Delta\sigma_r$	change in flow stress, $\sigma_2 - \sigma_1$

REFERENCES

1. Klein, M. J.; and Reid, C. N.: Strain Ageing, Metal Deformation Processing, Vol. I. DMIC Rep. 208, Battelle Memorial Inst., Aug. 14, 1964, pp. 114-126. (Available from DDC as AD-608 637.)

2. Keh, A. S.; Nakada, Y.; and Leslie, W. C.: Dynamic Strain Ageing in Iron and Steel. Dislocation Dynamics. A. R. Rosenfield, ed., McGraw-Hill Book Co., Inc., 1968, pp. 381-407.

3. Chang, W. H.: The Effect of Heat Treatment on Strength Properties of Molybdenum-Base Alloys. Trans. ASM, vol. 56, no. 1, Mar. 1963, pp. 107-124.

4. Chang, W. H.: Effect of Carbide Dispersion in Molybdenum Alloys. Trans. AIME, vol. 218, no. 2, Apr. 1960, pp. 254-256.

5. Chang, W. H.: Strain-Induced vs Pre-Existing Precipitation in the Mo-TZC Alloy. Trans. ASM, vol. 57, no. 2, June 1964, pp. 565-567.

6. Wilcox, B. A.; and Allen, B. C.: The Influence of Zirconium on Dynamic Strengthening of Niobium Alloys. J. Less Common Metals, vol. 13, no. 2, Aug. 1967, pp. 186-192.

7. Wilcox, B. A.: Basic Strengthening Mechanisms in Refractory Metals. Refractory Metal Alloys. I. Machlin, R. T. Begley and E. D. Weisert, eds., Plenum Press, 1968, pp. 1-39.

8. Glen, J.: The Effect of Alloying Elements on Creep Behavior. J. Iron Steel Inst., vol. 190, pt. 2, Oct. 1958, pp. 114-135.

9. Brindley, B. J.; and Barnby, J. T.: Dynamic Strain Ageing in Mild Steel. Acta Met., vol. 14, no. 12, Dec. 1966, pp. 1765- 1780.

10. Wilcox, B. A.; Gilbert, A.; and Allen, B. C.: Elevated Temperature Deformation and Fracture of a Precipitation Hardened Molybdenum Alloy. Sixth Metallwerk Plansee Seminar. Vol. 1. Metallwerk Plansee AG, Reutte, Austria, 1968.

11. Baird, J. D.; and Jamieson, A.: The Effects of Carbon, Nitrogen and Manganese on the High-Temperature Tensile Properties of Iron. Natl. Phys. Lab. Gt. Brit., Symp., vol. 15, no. 1, 1963, pp. 362-377.

12. Wilcox, B. A.; and Rosenfield, A. R.: On Serrated Yielding and Negative Strain-Rate Sensitivity. Mat. Sci. Eng., vol. 1, no. 4, Nov. 1966, pp. 201-205.

13. Baird, J. D.; and MacKenzie, C. R.: Effects of Nitrogen and Manganese on the Deformation Substructure of Iron Strained at 20°, 225°, and 450° C. J. Iron Steel Inst., vol. 202, pt. 5, May 1964, pp. 427-436.

14. Edington, J. W.; and Smallman, R. E.: The Relationship between Flow Stress and Dislocation Density in Deformed Vanadium. Acta Met., vol. 12, no. 12, Dec. 1964, pp. 1313-1328.

15. Rosen, A.; and Bodner, S. R.: The Influence of Strain Rate and Strain Ageing on the Flow Stress of Commercially-Pure Aluminum. J. Mech. Phys. Solids, vol. 15, no. 1, Jan. 1967, pp. 47-62.

16. Rosen, Abraham: Strain Ageing of Commercially Pure Aluminum. Mat. Sci. Eng., vol. 2, no. 3, Sept. 1967, pp. 117-124.

17. Naybour, R. D.: Hardening during Deformation of an 18Cr/12Ni/Nb Austenitic Steel at 650° C, Acta Met., vol. 13, no. 11, Nov. 1965, pp. 1197-1207.

18. Raffo, Peter L.: Exploratory Study of Mechanical Properties and Heat Treatment of Molybdenum-Hafnium-Carbon Alloys. NASA TN D-5025, 1969.

19. Fullman, R. L.; Carreker, R. P., Jr.; and Fisher, J. C.: Simple Devices for Approximating Constant Stress During Tensile Creep Tests. Trans. AIME, vol. 197, 1953, pp. 657-659.

20. Garofalo, F.; Richmond, O.; and Domis, W. F.: Design of Apparatus for Constant-Stress or Constant Load Creep Tests. J. Basic Eng., vol. 84, no. 2, June 1962, pp. 287-293.

21. Schoone, R. D.; and Fischione, E. A.: Automatic Unit for Thinning Transmission Electron Microscopy Specimens of Metals. Rev. Sci. Instr., vol. 37, no. 10, Oct. 1966, pp. 1351-1353.

22. Sherby, O. D.; and Burke, P. M.: Mechanical Behavior of Crystalline Solids at Elevated Temperature. Progress in Materials Science. Vol. 13, pt. 7. Bruce Chalmers, ed., Pergamon Press, 1968.

23. Askill, J.; and Tomlin, D. H.: Self-Diffusion in Molybdenum. Phil. Mag., vol. 8, no. 90, June 1963, pp. 997-1001.

24. Armstrong, Philip E.; and Brown, Harry L.: Dynamic Young's Modulus Measurements Above 1000° C on Some Pure Polycrystalline Metals and Commercial Graphites. Trans. AIME, vol. 230, no. 5, Aug. 1964, pp. 962-966.

25. Schmidt, F. F.; and Ogden, H. R.: The Engineering Properties of Molybdenum and Molybdenum Alloys. DMIC Rep. 190, Battelle Memorial Inst., Sept. 20, 1963. (Available from DDC as AD-426264.)

26. Conway, J. B.; and Flagella, P. N.: High-Temperature Reactor Materials Research. AEC Fuels and Materials Development Program Progress Report No. 67. Rep. GEMP-67, General Electric Co., June 30, 1967, pp. 11-42.

27. McLean, D.: The Physics of High Temperature Creep in Metals. Reports on Progress in Physics. Vol. 29, Pt. 1. A. C. Stickland, ed., Inst. Phys. and Phys. Soc., London, 1966, pp. 1-33.

28. Owen, W. S.; and Roberts, M. J.: Dynamic Ageing Effects in Iron-Nickel-Carbon Martensites. Dislocation Dynamics. A. R. Rosenfield, ed., McGraw-Hill Book Co., Inc., 1968, pp. 357-378.

29. Keh, A. S.; and Weissman, S.: Deformation Substructure in Body-Centered Cubic Metals. Electron Microscopy and the Strength of Crystals. Interscience Publ., 1963, pp. 231-300.

30. Li, J. C. M.: A Dislocation Mechanism of Transient Creep. Acta Met., vol. 11, no. 11, Nov. 1963, pp. 1269-1270.

31. Christian, J. W.: The Theory of Transformations in Metals and Alloys. Pergamon Press, 1966, pp. 430-431.

32. Ansell, G. S.: The Mechanism of Dispersion Strengthening - A Review. Oxide Dispersion Strengthening. George S. Ansell, Thomas D. Cooper, and Fritz V. Lenel, eds., Gordon-Breach Science Publ., 1968.

33. Ishida, Y.; and McLean, D.: Effect of Nitrogen and Manganese on Recovery Rate and Friction Stress During Creep of Iron. J. Iron Steel Inst., vol. 205, pt. 1, Jan. 1967, pp. 88-93.

NASA-Langley, 1969 — 17 E-4669